BAND MODEL FORMULATION FOR INHOMOGENEOUS OPTICAL PATHS

Stephen J. Young

Aerospace Corporation

Prepared for:

Defense Advanced Research Projects Agency

19 December 1974

This research was supported by the Defense Advanced Research Projects Agency of the Department of Defense and was monitored by Space and Missile Systems Organization (SAMSO) under Contract No. F04701-74-C-0075.

Approved

S. Siegel, Director
Chemistry and Physics Laboratory

Approval of this report does not constitute Air Force approval of the report's findings or conclusions. It is published only for the exchange and stimulation of ideas.

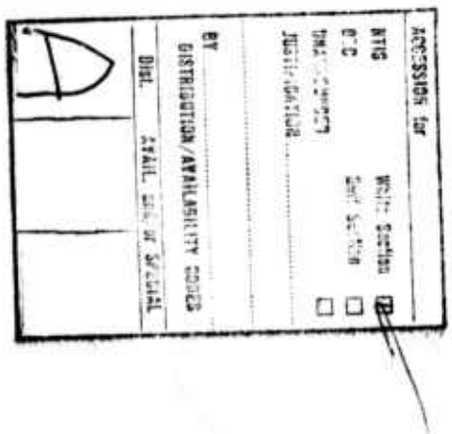

GERHARD E. AICHINGER
Acting Chief, Contracts Management Ofc

ib

UNCLASSIFIED

SECURITY CLASSIFICATION OF THIS PAGE (When Data Entered)

REPORT DOCUMENTATION PAGE		READ INSTRUCTIONS BEFORE COMPLETING FORM
1. REPORT NUMBER SAMSO-TR-74-255	2. GOVT ACCESSION NO.	3. RECIPIENT'S CATALOG NUMBER AD/A-003 403
4. TITLE (and Subtitle) BAND MODEL FORMULATION FOR INHOMOGENEOUS OPTICAL PATHS		5. TYPE OF REPORT & PERIOD COVERED Interim 6. PERFORMING ORG. REPORT NUMBER TR-0075(5647)-4
7. AUTHOR(s) Stephen J. Young		8. CONTRACT OR GRANT NUMBER(s) F04701-74-C-0075
9. PERFORMING ORGANIZATION NAME AND ADDRESS The Aerospace Corporation El Segundo, Calif. 90245		10. PROGRAM ELEMENT, PROJECT, TASK AREA & WORK UNIT NUMBERS
11. CONTROLLING OFFICE NAME AND ADDRESS Defense Advanced Research Projects Agency 1400 Wilson Blvd. Arlington, Va. 22209		12. REPORT DATE 19 December 1974 13. NUMBER OF PAGES
14. MONITORING AGENCY NAME & ADDRESS(if different from Controlling Office) Space and Missile Systems Organization Air Force Systems Command Los Angeles, Calif. 90045		15. SECURITY CLASS. (of this report) Unclassified 15a. DECLASSIFICATION/DOWNGRADING SCHEDULE

16. DISTRIBUTION STATEMENT (of this Report)

Approved for public release; distribution unlimited.

17. DISTRIBUTION STATEMENT (of the abstract entered in Block 20, if different from Report)

18. SUPPLEMENTARY NOTES

19. KEY WORDS (Continue on reverse side if necessary and identify by block number)

Band Model Formulation
Atmospheric Transmittance
High-Temperature Emission Sources
Exhaust Plume Emission

20. ABSTRACT (Continue on reverse side if necessary and identify by block number)

The band model formulation developed by Lindquist and Simmons to handle radiance calculations for highly inhomogeneous and nonisothermal optical paths is discussed and extended. The original formulation was based on the statistical band model for a random array of equal-intensity pressure-broadened Lorentz lines. Here, the formulation is extended to include bands of constant-intensity Doppler lines and bands of Lorentz or Doppler lines with an exponential distribution of line strengths. Results are presented for the equivalent width derivative functions $y(x, \rho)$ for the constant-intensity

DD FORM 1473 (FACSIMILE)

UNCLASSIFIED

SECURITY CLASSIFICATION OF THIS PAGE (When Data Entered)

19. KEY WORDS (Continued)

20. ABSTRACT (Continued)

Lorentz, constant-intensity Doppler, and exponential-intensity Doppler cases. Various approximations to these functions for extreme x and ρ conditions are also presented. A closed-form solution for $y(x, \rho)$ is given for the exponentially distributed Lorentz line case.

CONTENTS

FIGURES

TABLES

I. INTRODUCTION

Lindquist and Simmons[1] recently published a band model formulation designed to handle radiance calculations for highly inhomogeneous and non-isothermal optical paths. An important example of a case for which a high degree of inhomogeneity* pervails is the treatment of the propagation of infrared radiation from aircraft and missile plumes through long atmospheric paths. In many cases, the primary radiating species of the hot gaseous plume are H_2O and CO_2, and the primary atmospheric absorbers are these same species. The high degree of line position correlation between the hot gas emission spectrum and the cool gas absorption spectrum precludes the decoupling of the optical path into a source region and an absorbing region and performing a simple multiplication of the source band radiance by the atmospheric band transmittance to arrive at the transmitted radiance at a sensor position. The entire optical path, beginning at the sensor position and continuing through the cool intervening atmosphere and the hot gas source region, must be treated as a single radiating-absorbing media, i.e., calculations must be performed on a single highly inhomogeneous optical path.

The original formulation by Lindquist and Simmons[1] considered the case of a band of randomly arranged pressure-broadened Lorentz lines of equal intensity. The conditions for which a standard treatment of inhomogeneous paths with the Curtis-Godson approximation was likely to fail were determined, and the success achieved by the new formulation for these conditions was demonstrated. Here, this band model formulation is extended to a randomly arranged band of Lorentz lines distributed exponentially in line strength and a randomly arranged band of Doppler lines for both constant and exponential line strength distributions.

*An optical path is called inhomogeneous whenever a gradient in species concentration, pressure, or temperature exists along the path.

II. RADIANCE EQUATIONS

The mean radiance in a spectral interval $\Delta\nu$ centered on ν for a general optical path extending from $s = 0$ to $s = s_0$ is[2, 3]

$$\bar{L}(\nu) = -\int_0^{s_0} L^*(\nu, s) \frac{d\bar{\tau}(\nu, s)}{ds} ds \quad , \tag{1}$$

where $L^*(\nu, s)$ is the Planck radiation function evaluated at the temperature $T(s)$, and $\bar{\tau}(\nu, s)$ is the mean transmittance between the origin ($s = 0$) and the path position s. This expression is exact to the extent that $L^*(\nu, s)$ is sensibly constant over $\Delta\nu$. Practical radiance calculations are generally performed numerically by using the finite-difference form of the equation

$$\bar{L}(\nu) = -\sum_{i=1}^{N} L^*(\nu, s_i) \left[\bar{\tau}(\nu, s_i) - \bar{\tau}(\nu, s_{i-1})\right] \quad ,$$

and band model approximations for the transmittance function $\bar{\tau}(\nu, s)$.

Only a single optically active specie along the optical path is considered in this paper. If more than one active specie is present, the band transmittance function $\bar{\tau}(\nu, s)$ can be written as a product of the band transmittances of the individual species provided that the positions of lines in $\Delta\nu$ between any two species are uncorrelated. Then, the general band radiance equation can be written

$$\bar{L}(\nu) = -\int_0^{s_0} L^*(\nu, s)\, \bar{\tau}(\nu, s) \sum_{i=1}^{m} \frac{1}{\bar{\tau}_i(\nu, s)} \frac{d\,\bar{\tau}_i(\nu, s)}{ds} ds \quad ,$$

where

$$\bar{\tau}(\nu, s) = \prod_{i=1}^{m} \bar{\tau}_i(\nu, s)$$

and m is the number of active species.

Within the statistical band model formulation for an array of randomly arranged lines, the band transmittance for a single specie can be written as [2, 3]

$$\bar{\tau}(\nu, s) = e^{-\bar{W}(s)/\delta} \quad , \tag{2}$$

where $\bar{W}(s)$ is the mean equivalent width of all the lines in $\Delta\nu$, and δ is the mean line spacing in $\Delta\nu$. In order to provide a working model for transmittance calculations, $\bar{W}(s)$ is generally computed by assuming an approximate form for the distribution of line strengths S for the lines within $\Delta\nu$. If $P(S, \bar{S})dS$ is the probability that a randomly selected line has a strength S in dS when the mean line strength in $\Delta\nu$ is $\bar{S}$, then

$$\bar{W}(s, \bar{S}) = \int_0^\infty P(S, \bar{S})\, W(s, S)\, dS \quad ,$$

where $W(s, S)$ is the equivalent width of a single isolated line of strength S.

III. HOMOGENEOUS PATHS

The equivalent width functions W for isolated lines of both Lorentz and Doppler shapes as well as the mean equivalent width function $\overline{W}$ for these same line shapes and various assumed line strength distributions have been studied extensively for the case of homogeneous optical paths.[2-5] The cases of interest to the present work are:

1. Isolated Lorentz Line

$$W_L = 2\pi \gamma_L f(x_L) \quad , \tag{3a}$$

γ_L = Lorentz half-width at half-height ,

$$f(x) = xe^{-x}\left[J_0(ix) - iJ_1(ix)\right] \quad , \tag{3b}$$

J_n = Bessel functions of the first kind of order n ,

$$x_L = Su/2\pi\gamma_L \quad , \tag{3c}$$

u = optical depth of the path .

2. Band of Constant-Intensity Lorentz Lines

$$P(S, \overline{S}) = \delta(S - \overline{S}) \quad , \tag{4a}^*$$

$$\frac{\overline{W}_L}{\delta} = \beta_L f(x_L) \quad , \tag{4b}$$

$$\beta_L = 2\pi\overline{\gamma}_L/\delta_e \quad , \tag{4c}$$

*This δ is the dirac delta function, not the mean line spacing parameter.

δ_e = effective mean line spacing in $\Delta\nu$, (4d)

$\overline{\gamma}_L$ = average Lorentz line width in $\Delta\nu$, (4e)

$$x_L = \overline{k}u/\beta_L \quad , \tag{4f}$$

$$\overline{k} = \overline{S}/\delta_e \quad . \tag{4g}$$

3. Band of Exponentially Distributed Lorentz Lines

$$P(S, \overline{S}) = \overline{S}^{-1} e^{-S/\overline{S}} \quad , \tag{5a}$$

$$\frac{\overline{W}_L}{\delta} = \beta_L f_e(x_L) \quad , \tag{5b}$$

$$f_e(x) = x/\sqrt{1 + 2x} \quad . \tag{5c}$$

4. Isolated Doppler Line

$$W_D = \sqrt{\frac{\pi}{\ln 2}}\, \gamma_D g(x_D) \quad , \tag{6a}$$

γ_D = Doppler half-width at half-height ,

$$g(x) = \frac{2}{\sqrt{\pi}} \int_0^\infty \left\{ 1 - \exp\left[-xe^{-z^2} \right] \right\} dz \quad , \tag{6b}$$

$$= \sum_{n=0}^{\infty} \frac{(-1)^n x^{n+1}}{(n+1)!\sqrt{1+n}} \quad , \tag{6c}$$

$$x_D = \sqrt{\frac{\ln 2}{\pi}}\, \frac{Su}{\gamma_D} \quad . \tag{6d}$$

5. Band of Constant-Intensity Doppler Lines

$$\frac{\overline{W}_D}{\delta} = \beta_D \, g(x_D) \quad , \tag{7a}$$

$$\beta_D = \sqrt{\frac{\pi}{\ln 2}} \; \frac{\overline{\gamma}_D}{\delta_e} \quad , \tag{7b}$$

$$\overline{\gamma}_D = \text{average Doppler line width in } \Delta\nu \quad , \tag{7c}$$

$$x_D = \overline{k} u / \beta_D \quad . \tag{7d}$$

6. Band of Exponentially Distributed Doppler Lines

$$\frac{\overline{W}_D}{\delta} = \beta_D \, g_e(x_D) \quad , \tag{8a}$$

$$g_e(x) = \int_0^\infty e^{-z} \, g(xz) \, dz \quad , \tag{8b}$$

$$= \sum_{n=0}^{\infty} \frac{(-1)^n x^{n+1}}{\sqrt{1+n}} \qquad (x \le 1 \text{ only}) \quad . \tag{8c}$$

The function f(x) is the Ladenburg-Reiche function. Simple approximations to this function have been discussed by Goldman.[6] An accurate series expansion of about seven terms for large and small x for both f(x) and g(x) has been given by Rodgers and Williams.[7]* The function $g_e(x)$ has been studied by Malkmus,[5] who has given a series solution for small x and an asymptotic expansion for large x.

*The summation term in the large x expression for f(x) in Ref. (7) should be $b_n a^{-n}$.

The parameter δ_e entering in these expressions is the effective mean line spacing parameter and is not necessarily the same as the mean line spacing parameter δ. The form of the parameter δ_e depends on the intensity distribution function assumed and is introduced to yield the correct limit for $\overline{W}_L/\delta$ in the limit of strong line absorption.

IV. INHOMOGENEOUS PATHS

A standard procedure for extending the band model results for homogeneous paths to inhomogeneous paths for the case of the Lorentz line shape is the Curtis-Godson approximation.[3] The net effect of this procedure for isolated lines is to replace the line strength and line width parameters S and γ_L that appear in the expression for W_L with appropriate path-averaged values of these parameters. For a band of lines, path-averaged values of $\bar{k}$ and β_L are used in the expression for $\bar{W}_L$. The use of path-averaged values in the expression for the equivalent width for any line shape is referred to here as the Curtis-Godson approximation. The path-average definitions for an optical path that contains a single optically active specie for an isolated line are

$$S_e(s) = \frac{1}{u(s)} \int_0^s c(s')p(s')S(s')\,ds' \quad , \tag{9a}$$

$$\gamma_{eL}(s) = \frac{1}{u(s)S_e(s)} \int_0^s c(s')p(s')S(s')\gamma_L(s')\,ds', \tag{9b}$$

$$\gamma_{eD}(s) = \frac{1}{u(s)S_e(s)} \int_0^s c(s')p(s')S(s')\gamma_D(s')\,ds' \quad , \tag{9c}$$

$$x_L(s) = \frac{S_e(s)u(s)}{2\pi\gamma_{eL}(s)} \quad , \tag{9d}$$

$$x_D(s) = \sqrt{\frac{\ln 2}{\pi}}\,\frac{S_e(s)\,u(s)}{\gamma_{eD}(s)} \quad . \tag{9e}$$

For bands of lines, they are

$$\bar{k}_e(s) = \frac{1}{u(s)} \int_0^s c(s')p(s')\bar{k}(s')\,ds' \quad , \tag{10a}$$

$$\beta_{eL}(s) = \frac{1}{u(s)\bar{k}_e(s)} \int_0^s c(s')p(s')\bar{k}(s')\beta_L(s')\,ds' \quad , \tag{10b}$$

$$\beta_{eD}(s) = \frac{1}{u(s)\bar{k}_e(s)} \int_0^s c(s')p(s')\bar{k}(s')\beta_D(s')\,ds' \quad , \tag{10c}$$

$$x_L(s) = \bar{k}_e(s)u(s)/\beta_{eL}(s) \quad , \tag{10d}$$

$$x_D(s) = \bar{k}_e(s)u(s)/\beta_{eD}(s) \quad . \tag{10e}$$

The function u(s) is the optical depth

$$u(s) = \int_0^s c(s')p(s')ds' \quad ,$$

where p(s) is the total pressure, and c(s) is the mole fraction of the active gas at the path position s.

The essence of the Curtis-Godson approximation is to use path-averaged values in the expressions for the equivalent widths W and $\bar{W}$. Equivalently, through equation (2), this substitution of averaged values is made directly in the expression for the band transmittance function $\bar{\tau}(\nu, s)$. As pointed out by Lindquist and Simmons,[1] however, it is not $\bar{\tau}(\nu, s)$ that appears directly in the band radiance equation (1), but rather the derivative of the transmittance $d\bar{\tau}(\nu, s)/ds$. They concluded that, if approximations have

to be made, better accuracy could be obtained by making approximations to the transmittance derivative function rather than to the transmittance function itself.

From equation (2), the transmittance derivative is

$$\frac{d\bar{\tau}(\nu, s)}{ds} = - \bar{\tau}(\nu, s) \frac{1}{\delta} \frac{d\bar{W}(s)}{ds}$$

The approximation of the transmittance derivative thus depends on the approximation of the mean equivalent width derivative $d\bar{W}(s)/ds$ and a numerical integration of $d\bar{W}(s)/ds$ to obtain $\bar{W}(s)$. Then $\bar{\tau}(\nu, s)$ can be obtained from equation (2) and, finally, $d\bar{\tau}(\nu, s)/ds$ evaluated for use in equation (1). This expression for the transmittance derivative is obtained simply by differentiating the statistical band model expression for the mean transmittance. By starting from first principles for a random array of spectral lines (see Ref. 3 for example), however, it can be shown that the mean value of the transmittance derivative in $\Delta\nu$ is given by the same expression, i.e.,

$$\overline{\frac{d\tau(\nu, s)}{ds}} = \frac{d\bar{\tau}(\nu, s)}{ds} \quad .$$

As for $\bar{W}(s)$, the approximation to $d\bar{W}(s)/ds$ can begin with an examination of the equivalent width derivative for isolated lines. The definition of the equivalent width of an isolated spectral ine for a general optical path is[3]

$$W(s) = \int_{-\infty}^{\infty} \left\{ 1 - \exp\left[-\int_0^s c(s')p(s')k(\nu, s')ds' \right] \right\} d\nu \quad , \qquad (11)$$

where $k(\nu, s)$ is the spectral absorption coefficient of the line evaluated at path position s. The equivalent width derivative is thus

$$\frac{dW(s)}{ds} = c(s)p(s) \int_{-\infty}^{\infty} k(\nu, s) \exp\left[-\int_0^s c(s')p(s')k(\nu, s')ds' \right] ds \quad , \quad (12)$$

The spectral absorption coefficient for general line shapes depends on the line strength S(s) and width $\gamma(s)$. If S(s) and $\gamma(s)$ were replaced throughout equation (12) by the path-averaged values $S_e(s)$ and $\gamma_e(s)$, respectively, the result would be the Curtis-Godson approximation. The Lindquist-Simmons approximation is carried out by substituting the path-averaged values $S_e(s)$ and $\gamma_e(s)$ into only part of the expression given by equation (12). Specifically, $S_e(s)$ and $\gamma_e(s)$ are substituted only into the $k(\nu, s')$ term that appears in the exponential factor.

A. ISOLATED LINES

The case for the Lorentz line shape was considered by Lindquist and Simmons.[1] The spectral absorption coefficient for this line shape is

$$k_L(\nu, s) = \frac{S(s)}{\pi} \frac{\gamma_L(s)}{(\nu - \nu_0)^2 + \gamma_L^2(s)} , \tag{13}$$

where ν_0 is the line center. Substitution of equation (13) into (12) gives

$$\frac{dW_L(s)}{ds} = c(s)p(s) \frac{S(s)}{\pi} \int_{-\infty}^{\infty} \left\{ \frac{\gamma_L(s)}{\gamma_L^2(s) + (\nu - \nu_0)^2} \right\}$$

$$\times \exp \left\{ -\frac{1}{\pi} \int_0^s \frac{c(s')p(s')S(s')\gamma_L(s')}{\gamma_L^2(s') + (\nu - \nu_0)^2} \, ds' \right\} d(\nu - \nu_0) .$$

Substitution of $\gamma_{eL}(s)$ for $\gamma_L(s')$ in the exponential term* and use of the definitions for S_e [equation (9a)] and x_L [equation (9d)] yields

*The same result occurs also if $\gamma_{eL}(s)$ is subsituted for $\gamma_L(s')$ in only the denominator of the exponential term.

$$\frac{dW_L(s)}{ds} = c(s)p(s)\frac{S(s)}{\pi}\int_{-\infty}^{\infty}\left\{\frac{\gamma_L(s)}{\gamma_L^2(s) + (\nu - \nu_0)^2}\right\}$$

$$\times \exp\left\{-\frac{2x_L(s)\gamma_{eL}^2(s)}{\gamma_{eL}^2(s) + (\nu - \nu_0)^2}\right\} d(\nu - \nu_0) \quad .$$

By noting that the integral is even with respect to the integration over $\nu - \nu_0$, and making the substitution $\tan(\theta/2) = (\nu - \nu_0)/\gamma_{eL}$, the final result can be written as

$$\frac{dW_L(s)}{ds} = c(s)p(s)S(s)y_L(x_L, \rho_L) \quad , \tag{14a}$$

where

$$y_L(x, \rho) = \frac{2\rho}{\pi}\int_0^{\pi} \frac{e^{-x(1 + \cos\theta)}}{(\rho^2 + 1) + (\rho^2 - 1)\cos\theta} d\theta \quad , \tag{14b}$$

and where $\rho_L = \gamma_L(s)/\gamma_{eL}(s)$. The parameter ρ_L is the ratio of the local value of the line width to the path-averaged value of the line width up to that local point and is the primary index of the degree of inhomogeneity prevailing at postion s.

For an isolated Dopper line, the spectral absorption coefficient is

$$k_D(\nu, s) = \sqrt{\frac{\ln 2}{\pi}}\ \frac{S(s)}{\gamma_D(s)}\, e^{-\ln 2(\nu - \nu_0)^2/\gamma_D^2(s)} \quad . \tag{15}$$

By following a procedure similar to that for the Lorentz line, the equivalent width derivative can be derived as

$$\frac{dW_D(s)}{ds} = c(s)p(s)S(s)y_D(x_D, \rho_D) \quad , \tag{16a}$$

where

$$y_D(x, \rho) = \frac{2}{\sqrt{\pi}} \int_0^\infty e^{-z^2 - xe^{-\rho^2 z^2}} dz \quad , \tag{16b}$$

and

$$\rho_L = \gamma_D(s)/\gamma_{eD}(s) \quad .$$

B. BANDS OF LINES

The derivative of the mean equivalent width is obtained from the derivatives for isolated lines by applying the distribution functions $P(S, \bar{S})$ given by equations (4a) and (5a). The application of these distribution functions is not, however, as clearly defined as for their application to W for homogeneous paths. The derivative expressions of equations (14) and (16) depend not only on the local line strength $S(s)$, but also on the path-averaged line strength $S_e(s)$. Thus, both $S(s)$ and $S_e(s)$ could presumably have distributions about mean values $\bar{S}(s)$ and $\bar{S}_e(s)$, respectively. Ideally, the averaging should be done with a distribution function of the form $P(S, \bar{S}, S_e, \bar{S}_e)$. One possibility would be to write

$$P(S, \bar{S}, S_e, \bar{S}_e) = P_1(S, \bar{S})\, P_2(S_e, \bar{S}_e)$$

so that independent distributions could be applied to S and S_e. However, this form implies a complete independence of the variables S and S_e. This is clearly unrealistic because S_e is defined as the average value of S. Rather than assuming the complete independence of S and S_e, the present approach is to assume the opposite extreme, i.e., that S and S_e are completely dependent. Although this situation is probably not fulfilled either, it is certainly much more realistic than the assumption of independence. The assumption of complete dependence is equivalent to the assumption that, for each line in $\Delta\nu$,

$$S_e^i(s) = C(s)S^i(s), \tag{17}$$

where C(s) is a constant independent of the line index i. Since the only variation of $S^i(s)$ along an optical path is with temperature, this assumption implies that all lines in $\Delta\nu$ have the same temperature dependence. Since C(s) is independent of i, equation (17) also applies to the average line $\bar{S}(s)$. Thus, $\bar{S}_e(s) = C(s)\bar{S}(s)$. The mean equivalent width derivative is then evaluated according to

$$\overline{\frac{dW(s,S)}{ds}} = \int_0^\infty P(S,\bar{S}) \frac{dW(s,S)}{ds}\, dS \quad , \tag{18}$$

where the S_e term in dW/ds is replaced by C(s)S. Note that this quantity is the mean value of the equivalent width derivative and not the derivative of the mean equivalent width, although it is to be considered as such when computing $d\bar{\tau}/ds$ or $\bar{W}$ by numerical integration.

The result of substituting equation (14a) into (18) and performing the integration over S for the constant-line-intensity distribution function [equation (4a)] is

$$\frac{1}{\delta} \overline{\frac{dW_L(s)}{ds}} = c(s)p(s)\bar{k}(s)y_L(\bar{x}_L, \rho_L) \quad , \tag{19}$$

where $y_L(x, \rho)$ is the same function as given by equation (14b), $\bar{x}_L = \bar{k}_e(s)u(s)/\beta_{eL}(s)$ and $\rho_L = \beta_L(s)/\beta_{eL}(s)$. For a band of constant-intensity Doppler lines, a similar procedure gives

$$\frac{1}{\delta}\frac{\overline{dW_D(s)}}{ds} = c(s)p(s)\bar{k}(s)y_D(\bar{x}_D, \rho_D) \quad , \tag{20}$$

where $y_D(x, \rho)$ is the same function as given by equation (16b), $\bar{x}_D = \bar{k}_e(s)u(s)/\beta_{eD}(s)$ and $\rho_D = \beta_D(s)/\beta_{eD}(s)$. For an exponential distribution of line strengths for Lorentz lines, a similar procedure in which the intensity distribution function of equation (5a) is used gives

$$\frac{1}{\delta}\frac{\overline{dW_L(s)}}{ds} = c(s)p(s)\bar{k}(s)\bar{y}_L(\bar{x}_L, \rho_L) \quad , \tag{21a}$$

where

$$\bar{y}_L(x, \rho) = \frac{2\rho}{\pi}\int_0^{\pi} \frac{d\theta}{[(\rho^2 + 1) + (\rho^2 - 1)\cos\theta][1 + x(1 + \cos\theta)]^2} \tag{21b}$$

For an exponential distribution of line strengths for Doppler lines,

$$\frac{1}{\delta}\frac{\overline{dW_D(s)}}{ds} = c(s)p(s)\bar{k}(s)\bar{y}_D(\bar{x}_D, \rho_D) \quad , \tag{22a}$$

where

$$\bar{y}_D(x, \rho) = \frac{2}{\sqrt{\pi}}\int_0^{\infty} \frac{e^{-z^2}}{\left[1 + xe^{-\rho^2 z^2}\right]^2}\, dz \quad . \tag{22b}$$

C. DISCUSSION

In the Curtis-Godson approximation, the substitution of path-averaged values in the expression for the equivalent width, or throughout the expression for the derivative of the equivalent width, results in a complete separation of the spectral and spatial integration operations. In all cases for the Lindquist-Simmons approximation, these coordinates are not separated. This result is demonstrated by the fact that, for each new path coordinate s, $y(\mathbf{x}, \rho)$ must be recomputed by a θ or z integration. Except for the case of $\bar{y}_L$ for an exponential line strength distribution, closed-form solutions for the $y(x, \rho)$ functions have not been found. In a practical application of the formulation, the numerical reevaluation of $y(x, \rho)$ for each new path position could conceivably be excessively time consuming even for computer application. The approach taken in the calculation of $y(x, \rho)$ for practical application has been to perform interpolations with respect to x and ρ on a table of precomputed values of $y(\mathbf{x}, \rho)$. The equivalent width derivative functions $y_L(x, \rho)$, $y_D(x, \rho)$, and $\bar{y}_D(\mathbf{x}, \rho)$ are presented in Tables 1, 2, and 3, respectively. The functions are also presented graphically in Figs. 1b, 3b, and 4b, respectively, as functions of x for various values of ρ. Details of the numerical integration of these functions, simple approximations to these functions for limiting values of x and ρ, and the closed-form solution of $\bar{y}_L(x, \rho)$ for an exponential intensity distribution are presented in Section V.

Inspection of the general equation

$$\frac{dW}{ds} = c(s)p(s)S(s)y(x, \rho)$$

forces the following physical restrictions to be placed on the function y with respect to the parameter x.[1] For small x, the equivalent width must grow linearly with x, i.e., as $x \to 0$, $y \to 1$. Since dW/ds can never increase faster than it does in the linear region, y must be a nonincreasing function with x (and hence $y \leq 1$ for all x). Clearly, y must also remain positive for all x. All of these features are evident for the $y(\mathbf{x}, \rho)$ computed in the

Table 1. Equivalent Width Derivative Function for an Isolated Lorentz Line or Band of Equal-Intensity Lorentz Lines

	ρ							
x	1.0E-03	2.0E-03	5.0E-03	1.0E-02	2.0E-02	5.0E-02	1.0E-01	2.0E-01
1.0E-03	.99801E+00	.99801E+00	.99801E+00	.99802E+00	.99804E+00	.99810E+00	.99818E+00	.99833E+00
2.0E-03	.99601E+00	.99602E+00	.99603E+00	.99605E+00	.99609E+00	.99620E+00	.99637E+00	.99667E+00
5.0E-03	.99006E+00	.99007E+00	.99010E+00	.99015E+00	.99024E+00	.99052E+00	.99095E+00	.99170E+00
1.0E-02	.98022E+00	.98024E+00	.98030E+00	.98039E+00	.98059E+00	.98114E+00	.98199E+00	.98349E+00
2.0E-02	.96083E+00	.96087E+00	.96098E+00	.96117E+00	.96155E+00	.96264E+00	.96432E+00	.96727E+00
5.0E-02	.90493E+00	.90502E+00	.90530E+00	.90576E+00	.90666E+00	.90926E+00	.91329E+00	.92037E+00
1.0E-01	.81890E+00	.81907E+00	.81959E+00	.82044E+00	.82211E+00	.82696E+00	.83447E+00	.84770E+00
2.0E-01	.67062E+00	.67091E+00	.67180E+00	.67327E+00	.67617E+00	.68457E+00	.69765E+00	.72080E+00
5.0E-01	.36837E+00	.36886E+00	.37031E+00	.37273E+00	.37751E+00	.39142E+00	.41331E+00	.45276E+00
1.0E+00	.13585E+00	.13637E+00	.13791E+00	.14047E+00	.14554E+00	.16046E+00	.18430E+00	.22848E+00
2.0E+00	.18689E-01	.19061E-01	.20179E-01	.22038E-01	.25745E-01	.36775E-01	.54838E-01	.89697E-01
5.0E+00	.24108E-03	.43677E-03	.10238E-02	.20022E-02	.39588E-02	.98266E-02	.19594E-01	.39043E-01
1.0E+01	.13143E-03	.26283E-03	.65707E-03	.13141E-02	.26282E-02	.65702E-02	.13137E-01	.26251E-01
2.0E+01	.90964E-04	.18193E-03	.45482E-03	.90963E-03	.18193E-02	.45480E-02	.90951E-02	.18183E-01
5.0E+01	.56850E-04	.11370E-03	.28425E-03	.56850E-03	.11370E-02	.28425E-02	.56847E-02	.11368E-01
1.0E+02	.40045E-04	.80091E-04	.20023E-03	.40045E-03	.80090E-03	.20023E-02	.40045E-02	.80082E-02
2.0E+02	.28263E-04	.56525E-04	.14131E-03	.28263E-03	.56525E-03	.14131E-02	.28262E-02	.56522E-02
5.0E+02	.17855E-04	.35709E-04	.89273E-04	.17855E-03	.35709E-03	.89273E-03	.17855E-02	.35709E-02
1.0E+03	.12620E-04	.25241E-04	.63102E-04	.12620E-03	.25241E-03	.63102E-03	.12620E-02	.25241E-02
2.0E+03	.89223E-05	.17845E-04	.44611E-04	.89223E-04	.17845E-03	.44611E-03	.89223E-03	.17844E-02
5.0E+03	.56423E-05	.11285E-04	.28212E-04	.56423E-04	.11285E-03	.28212E-03	.56423E-03	.11285E-02
1.0E+04	.39896E-05	.79791E-05	.19948E-04	.39896E-04	.79791E-04	.19948E-03	.39896E-03	.79791E-03

Table 1. Equivalent Width Derivative Function for an Isolated Lorentz Line or Band of Equal-Intensity Lorentz Lines (Continued)

	ρ							
x	5.0E-01	1.0E+00	2.0E+00	5.0E+00	1.0E+01	2.0E+01	5.0E+01	1.0E+02
1.0E-03	.99867E+00	.99900E+00	.99933E+00	.99967E+00	.99982E+00	.99990E+00	.99996E+00	.99998E+00
2.0E-03	.99734E+00	.99800E+00	.99867E+00	.99933E+00	.99964E+00	.99981E+00	.99992E+00	.99996E+00
5.0E-03	.99336E+00	.99502E+00	.99668E+00	.99834E+00	.99909E+00	.99953E+00	.99980E+00	.99990E+00
1.0E-02	.98678E+00	.99007E+00	.99338E+00	.99669E+00	.99819E+00	.99905E+00	.99961E+00	.99980E+00
2.0E-02	.97377E+00	.98030E+00	.98684E+00	.99341E+00	.99640E+00	.99811E+00	.99922E+00	.99961E+00
5.0E-02	.93603E+00	.95182E+00	.96775E+00	.98381E+00	.99115E+00	.99536E+00	.99809E+00	.99903E+00
1.0E-01	.87715E+00	.90710E+00	.93755E+00	.96852E+00	.98276E+00	.99095E+00	.99627E+00	.99812E+00
2.0E-01	.77299E+00	.82694E+00	.88272E+00	.94038E+00	.96724E+00	.98276E+00	.99288E+00	.99640E+00
5.0E-01	.54494E+00	.64504E+00	.75374E+00	.87179E+00	.92876E+00	.96228E+00	.98436E+00	.99208E+00
1.0E+00	.33767E+00	.46576E+00	.61609E+00	.79262E+00	.88275E+00	.93730E+00	.97383E+00	.98672E+00
2.0E+00	.18374E+00	.30851E+00	.47505E+00	.69858E+00	.82441E+00	.90443E+00	.95964E+00	.97944E+00
5.0E+00	.96025E-01	.18354E+00	.32521E+00	.56688E+00	.73185E+00	.84839E+00	.93430E+00	.96622E+00
1.0E+01	.65228E-01	.12783E+00	.23934E+00	.46561E+00	.64900E+00	.79338E+00	.90784E+00	.95211E+00
2.0E+01	.45329E-01	.89780E-01	.17340E+00	.36854E+00	.55676E+00	2557E+00	.87274E+00	.93290E+00
5.0E+01	.28389E-01	.56562E-01	.11149E+00	.25678E+00	.42905E+00	.61679E+00	.80955E+00	.89674E+00
1.0E+02	.20010E-01	.39944E-01	.79301E-01	.18941E+00	.33695E+00	.52381E+00	.74691E+00	.85867E+00
2.0E+02	.14127E-01	.28227E-01	.56245E-01	.13723E+00	.25574E+00	.42795E+00	.67102E+00	.80915E+00
5.0E+02	.89262E-02	.17846E-01	.35638E-01	.88194E-01	.17069E+00	.30894E+00	.55373E+00	.72366E+00
1.0E+03	.63098E-02	.12617E-01	.25216E-01	.62714E-01	.12326E+00	.23239E+00	.45832E+00	.64384E+00
2.0E+03	.44610E-02	.89212E-02	.17836E-01	.44473E-01	.88146E-01	.17060E+00	.36477E+00	.55364E+00
5.0E+03	.28211E-02	.56420E-02	.11282E-01	.28176E-01	.56145E-01	.11071E+00	.25541E+00	.42760E+00
1.0E+04	.19948E-02	.39895E-02	.79783E-02	.19935E-01	.39797E-01	.79016E-01	.18883E+00	.33621E+00

Table 2. Equivalent Width Derivative Function for an Isolated Doppler Line or Band of Equal-Intensity Doppler Lines

	ρ							
x	5.0E-01	6.0E-01	7.0E-01	8.0E-01	9.0E-01	1.0E+00	1.5E+00	2.0E+00
1.0E-02	.99110E+00	.99146E+00	.99184E+00	.99222E+00	.99260E+00	.99296E+00	.99447E+00	.99555E+00
2.0E-02	.98227E+00	.98300E+00	.98376E+00	.98451E+00	.98526E+00	.98597E+00	.98899E+00	.99112E+00
5.0E-02	.95628E+00	.95806E+00	.95991E+00	.96177E+00	.96360E+00	.96536E+00	.97279E+00	.97805E+00
1.0E-01	.91542E+00	.91795E+00	.92153E+00	.92513E+00	.92867E+00	.93210E+00	.94660E+00	.95690E+00
2.0E-01	.83648E+00	.84287E+00	.84956E+00	.85633E+00	.86301E+00	.86949E+00	.89713E+00	.91687E+00
5.0E-01	.64078E+00	.65364E+00	.66735E+00	.68142E+00	.69549E+00	.70927E+00	.76922E+00	.81286E+00
1.0E+00	.41251E+00	.43057E+00	.45040E+00	.47130E+00	.49265E+00	.51393E+00	.60975E+00	.68176E+00
2.0E+00	.17378E+00	.19204E+00	.21349E+00	.23740E+00	.26298E+00	.28946E+00	.41742E+00	.51991E+00
5.0E+00	.15646E-01	.23089E-01	.34215E-01	.49239E-01	.67884E-01	.89543E-01	.21819E+00	.34001E+00
1.0E+01	.75570E-03	.23452E-02	.59521E-02	.12474E-01	.22431E-01	.35878E-01	.13911E+00	.25659E+00
2.0E+01	.33319E-04	.26515E-03	.11797E-02	.35503E-02	.81782E-02	.15619E-01	.92613E-01	.19931E+00
5.0E+01	.67474E-06	.17107E-04	.15320E-03	.72684E-03	.22901E-02	.54769E-02	.55716E-01	.14578E+00
1.0E+02	.37342E-07	.22410E-05	.33786E-04	.22498E-03	.89503E-03	.25307E-02	.38444E-01	.11622E+00

Table 2. Equivalent Width Derivative Function for an Isolated Doppler Line or Band of Equal-Intensity Doppler Lines (Continued)

	ρ			
x	2.0E+00	5.0E+00	1.0E+01	2.0E+01
1.0E-02	.99555E+00	.99805E+00	.99901E+00	.99950E+00
2.0E-02	.99112E+00	.99611E+00	.99802E+00	.99901E+00
5.0E-02	.97805E+00	.99037E+00	.99511E+00	.99755E+00
1.0E-01	.95690E+00	.98107E+00	.99039E+00	.99518E+00
2.0E-01	.91687E+00	.96343E+00	.98144E+00	.99068E+00
5.0E-01	.81286E+00	.91729E+00	.95798E+00	.97891E+00
1.0E+00	.68176E+00	.85828E+00	.92792E+00	.96380E+00
2.0E+00	.51991E+00	.78315E+00	.88944E+00	.94444E+00
5.0E+00	.34001E+00	.69178E+00	.84199E+00	.92049E+00
1.0E+01	.25659E+00	.64116E+00	.81499E+00	.90677E+00
2.0E+01	.19931E+00	.60054E+00	.79254E+00	.89529E+00
5.0E+01	.14578E+00	.55414E+00	.76681E+00	.88[illegible]5E+00
1.0E+02	.11622E+00	.52386E+00	.74941E+00	.87304E+00
2.0E+02	.73219E-02	.49651E+00	.73335E+00	.86468E+00
5.0E+02	.36827E-02	.46394E+00	.71376E+00	.85442E+00
1.0E+03	.21898E-02	.44156E+00	.69996E+00	.84715E+00
2.0E+03	.13020E-02	.42083E+00	.68690E+00	.84023E+00
5.0E+03	.65489E-03	.39560E+00	.67062E+00	.83155E+00
1.0E+04	.38940E-03	.37796E+00	.65895E+00	.82529E+00

Table 3. Equivalent Width Derivative Function for an Exponential Intensity Distribution of Doppler Lines

	ρ					
x	5.0E-01	7.5E-01	1.0E+00	1.5E+00	2.0E+00	5.0E+00
1.0E-02	.98236E+00	.98421E+00	.98603E+00	.98903E+00	.99116E+00	.99612E+00
2.0E-02	.96518E+00	.96880E+00	.97239E+00	.97831E+00	.98250E+00	.99232E+00
5.0E-02	.91632E+00	.92486E+00	.93338E+00	.94756E+00	.95765E+00	.98138E+00
1.0E-01	.84290E+00	.85839E+00	.87410E+00	.90056E+00	.91956E+00	.96456E+00
2.0E-01	.72063E+00	.74643E+00	.77337E+00	.81987E+00	.85384E+00	.93534E+00
5.0E-01	.48066E+00	.52078E+00	.56603E+00	.64948E+00	.71327E+00	.87176E+00
1.0E+00	.28340E+00	.32630E+00	.38011E+00	.48899E+00	.57756E+00	.80829E+00
2.0E+00	.13310E+00	.16771E+00	.21874E+00	.33801E+00	.44458E+00	.74261E+00
5.0E+00	.35627E-01	.52793E-01	.87230E-01	.19370E+00	.30686E+00	.66702E+00
1.0E+01	.11015E-01	.18874E-01	.40111E-01	.12653E+00	.23433E+00	.62066E+00
2.0E+01	.31005E-02	.61956E-02	.17988E-01	.83937E-01	.18185E+00	.58159E+00
5.0E+01	.53566E-03	.13120E-02	.62300E-02	.50073E-01	.13275E+00	.53773E+00
1.0E+02	.13756E-03	.39103E-03	.28262E-02	.34402E-01	.10577E+00	.50878E+00
2.0E+02	.34865E-04	.11436E-03	.12979E-02	.23860E-01	.84834E-01	.48258E+00
5.0E+02	.56251E-05	.22103E-04	.47194E-03	.14865E-01	.63847E-01	.45133E+00
1.0E+03	.14102E-05	.63180E-05	.22189E-03	.10454E-01	.51718E-01	.42981E+00
2.0E+03	.35306E-06	.17970E-05	.10507E-03	.73811E-02	.42018E-01	.40984E+00
5.0E+03	.56537E-07	.33929E-06	.39459E-04	.46818E-02	.32049E-01	.38550E+00
1.0E+04	.14138E-07	.95905E-07	.18908E-04	.33280E-02	.26174E-01	.36846E+00

Lindquist-Simmons approximation (Figs. 1b, 2b, 3b, and 4b). In the Curtis-Godson approximation, the function $y(x, \rho)$ can be derived as

$$y(x, \rho) = (2 - \rho) \frac{dh(x)}{dx} + (\rho - 1) \frac{h(x)}{x} \quad , \tag{23}$$

where $h(x)$ is any one of the equivalent width functions $f(x)$, $f_e(x)$, $g(x)$, or $g_e(x)$ depending on line and distribution type considered. The functions $y(x, \rho)$ in the Curtis-Godson approximation are plotted in Figs. 1a, 2a, 3a, and 4a for comparison with the appropriate functions computed in the Lindquist-Simmons approximation. It is immediately evident that, for certain conditions of the parameters x and ρ, the physical restraints imposed on $y(x, \rho)$ are exceeded in the Curtis-Godson approximation. The dominant failure for all cases is that $y(x, \rho)$ exceeds unity for various ranges of x whenever the inhomogeneity factor is much greater than ~ 2. For any value of ρ, however, $y(x, \rho)$ eventually becomes less than unity for large enough x. Thus, the primary condition for failure of the Curtis-Godson approximation is the condition of a large inhomogeneity, resulting in a large value for ρ, existing near the beginning (small or medium x) of the optical path. This is the condition that would prevail, for example, in calculations for H_2O or CO_2 flame radiation propagation through a cool intervening atmosphere in a band wing region. If the condition for the failure of the Curtis-Godson approximation occurs at any time, the condition may be self-perpetuating because, although the dimensionless optical depth parameter x is a measure of depth into the optical path and generally increases with the geometric path parameter s, there are conditions for which x can decrease with increasing s. Differentiation of equation (9d), for example, yields

$$\frac{dx_L(s)}{ds} = \frac{c(s)p(s)\bar{k}(s)}{\beta_{eL}(s)}[2 - \rho_L(s)] \quad .$$

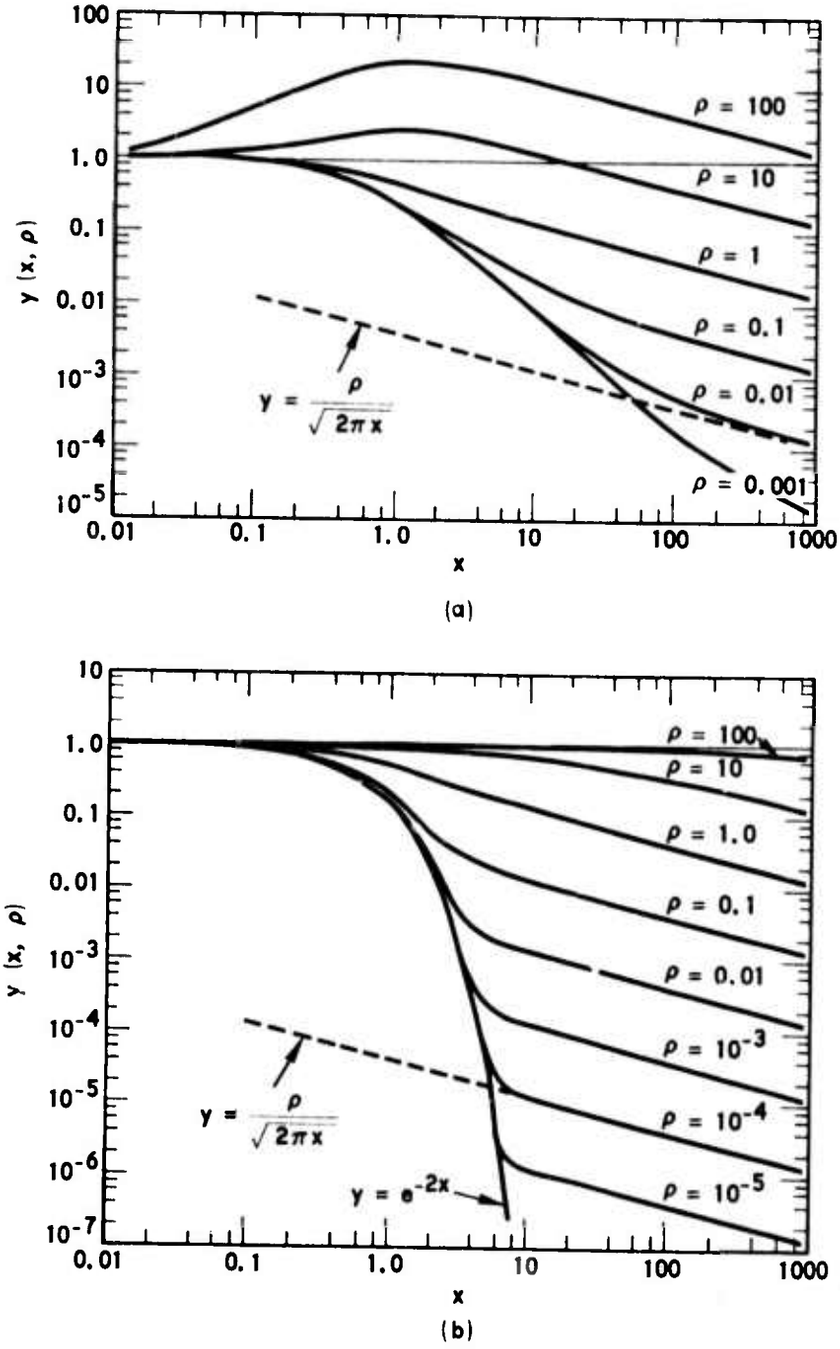

Figure 1. Equivalent Width Derivative Function for an Isolated Lorentz Line or Band of Equal-Intensity Lorentz Lines. (a) Curtis-Godson approximation; (b) Lindquist-Simmons approximation.

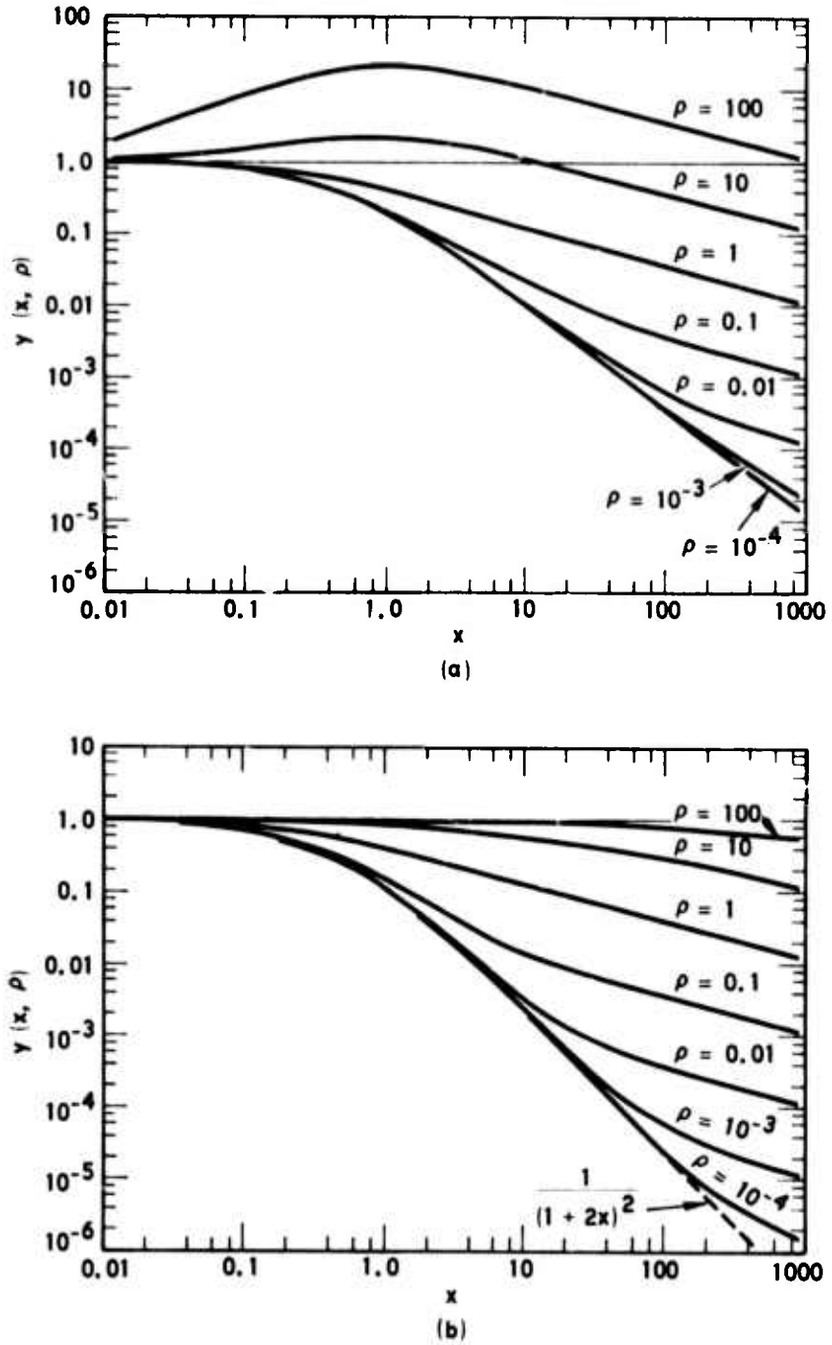

Figure 2. Equivalent Width Derivative Function for an Exponential Intensity Distribution of Lorentz Lines. (a) Curtis-Godson approximation; (b) Lin iquist-Simmons approximation.

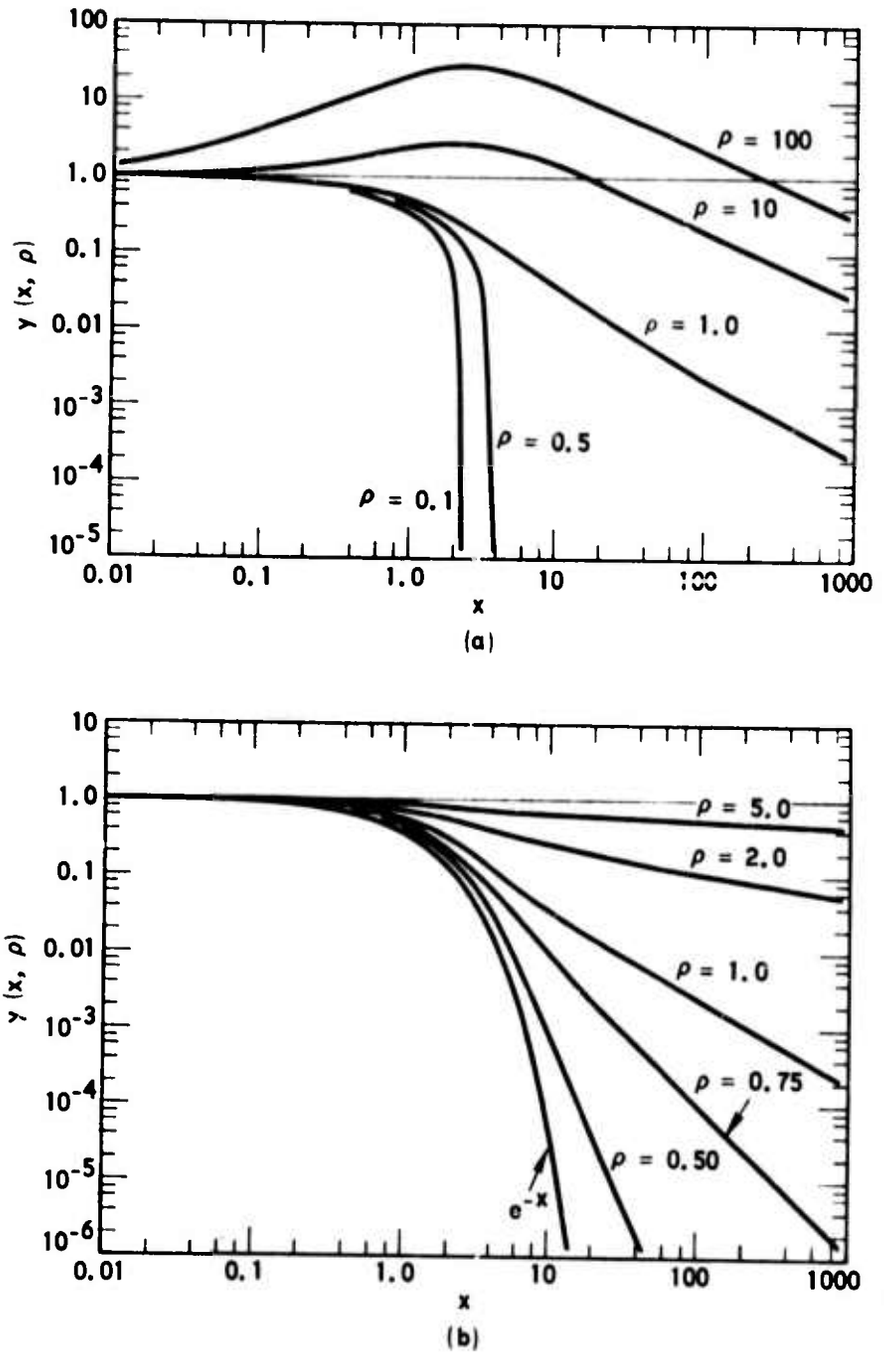

Figure 3. Equivalent Width Derivative Function for an Isolated Doppler Line or Band of Equal-Intensity Doppler Lines. (a) Curtis-Godson approximation; (b) Lindquist-Simmons approximation.

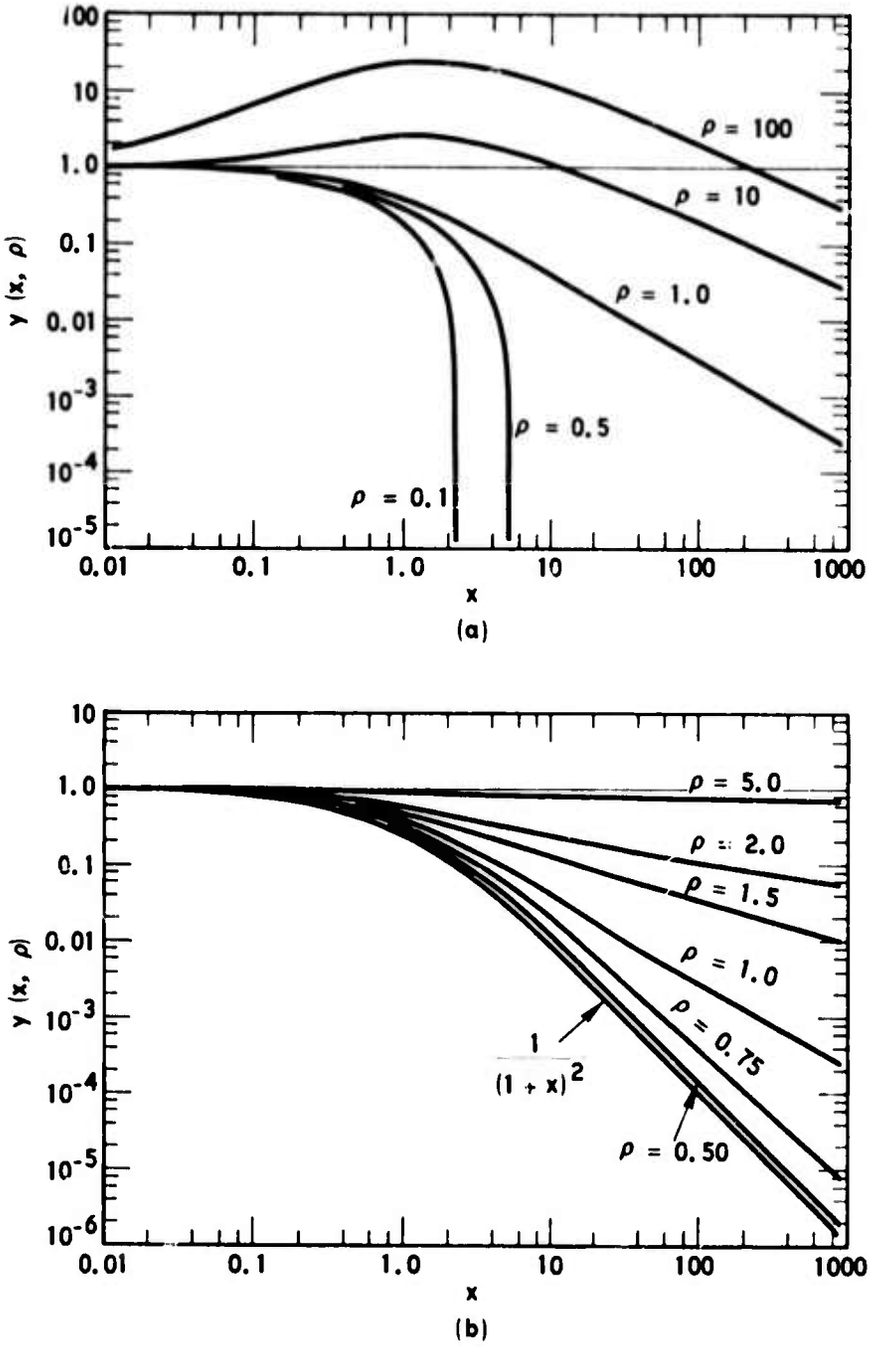

Figure 4. Equivalent Width Derivative Function for an Exponential Intensity Distribution of Doppler Lines. (a) Curtis-Godson approximation; (b) Lindquist-Simmons approximation.

Thus, whenever ρ is greater than 2, x_L decreases with increasing s and will not increase to a value where y is again less than unity. Another failure of the Curtis-Godson approximation occurs for Doppler lines where $y(x, \rho)$ becomes negative for certain values of ρ less than unity.

Certain other features of the results for the $y(x, \rho)$ functions should be discussed. In the Lindquist-Simmons approximation, the changeover from the small x to the large x form of the function generally occurs much more rapidly than in the Curtis-Godson approximation. This is most evident for $y_L(x, \rho)$ for small ρ (Fig. 1). For a given line shape within the Lindquist-Simmons approximation, the changeover from the small x to the large x form of the function is very much more rapid for the constant line-intensity distribution than for exponential distribution. This is in keeping with the same phenomenon observed for the changeover of $\overline{W}$ between the weak-line and strong-line regions and is explained by the allowance of weak lines by the exponential distribution function.[3,4]

The range of values of ρ for which Tables 1-3 were prepared reflect that the primary application of the formulation is to atmospheric transmittance problems that involve hot gaseous emission sources. The parameter ρ has the value unity at the beginning of any optical path. The variation of ρ along the path then depends on the path type and the variation of $\gamma(s)$ or $\beta(s)$ along the path. In application to atmospheric slant paths, two conditions prevail for pressure-broadened Lorentz lines. For an optical path that originates at a high altitude and progresses deeper into the atmosphere, ρ_L increases gradually and generally approaches a final value of ~2. For an optical path that originates low in the atmosphere and progresses upward to low-pressure regions, ρ_L may decrease to values as small as 10_{-7} (for an atmosphere cut-off altitude of 100 km, for example). Nearly all of this ρ_L variation is caused by the pressure variation of the line half-width given by

$$\gamma_L(s) = \gamma_L^0 p(s) \sqrt{\frac{273}{T(s)}} \quad ,$$

where γ_L^0 is the line-broadening parameter for standard temperature and pressure. Very little variation is due to the temperature variation of $\gamma_L(s)$ or of $\delta_e(s)$ because of the relative isothermality of the atmosphere. The Doppler half-width is

$$\gamma_D(s) = \nu_0 \sqrt{\frac{2kT}{m}} \ln 2$$

and is pressure independent. Thus, for a Doppler line, ρ_D will never vary much from unity for an atmospheric path.

For an optical path that progresses from a cool region into a hot region, β may increase substantially near the boundary of the region and result in local ρ values in excess of 100. Here, the primary cause of the increase in ρ is the strong temperature dependence of $\delta_e(s)$. For a hot gas, many more lines will generally be important in a spectral interval $\Delta\nu$ than for a cool gas. Consequently, the effective mean line spacing will be much smaller for the hot gas, and the β value will be much larger. The degree of inhomogeneity encountered in passing from a cool region into a hot region will be about the same for both Lorentz and Doppler lines because the major variation is in $\delta_e(s)$ rather than in the relatively less-sensitive square-root variation of half-width with temperature. The possibility of very small ρ values obtained by passing from a hot region into a cool region is formally allowed, but is not of much practical importance and, hence, is not considered here. This limitation has the practical advantage of not having to consider the evaluation of $y(x, \rho)$ for Doppler lines for values of ρ_D much smaller than the minimum value likely to be obtained for strictly atmospheric paths, i.e., about 0.5.

The variation of $y(x, \rho)$ with ρ also requires some discussion. The solutions for all of the $y(x, \rho)$ functions display the feature that $y(x, \rho)$ is nondecreasing as ρ increases and that $y \to 1$ as $\rho \to \infty$. For an isolated line, an increase in ρ to a large value at some point along the path means that the local value of the line width is larger than the width averaged over all of the previous path. If the local width is much wider than the averaged width, the

line will continue to grow essentially as a new line with only a small perturbation near the line center caused by the previous path. Thus, the equivalent width will grow nearly linearly with γ near unity. For a band of lines, the same effect with line width may occur or, as is more likely, the mean equivalent width will grow as a new band because of the addition of many new weak lines at the inhomogeneity, i.e., the increase in ρ is caused by a large decrease in δ_e rather than an increase in γ.

V. SOLUTIONS FOR $y(x, \rho)$ FUNCTIONS

A. NUMERICAL INTEGRATION OF $y_L(x, \rho)$

A straightforward numerical integration of equation (14b) was performed by dividing the region from $\theta = 0$ to $\theta = \pi$ into N equal sized intervals, integrating over each interval with a 12-point Wedle integration approximation,[8] and allowing N to increase until the desired accuracy was achieved for each fixed x and ρ. The data in Table 1 are accurate to at least 1 part in 10^5. Without some form of smoothing transformation, this integration procedure would not be practical for an in-program computer calculation of $y(x, \rho)$ for each new path coordinate s because, for certain extremes of x and ρ, the integrand becomes very sharply peaked about $\theta = 0$ or $\theta = \pi$ or both. Analysis of the integrand reveals that, for $x > (1 - \rho^2)/2\rho^2$, the integrand peaks around $\theta = \pi$; for $x < (1 - \rho^2)/2$, it peaks around $\theta = 0$; and for x between these limits, it peaks around both $\theta = 0$ and $\theta = \pi$. For extreme conditions of these cases, the integrand becomes highly concentrated in the regions of the peaks. Although detrimental to straightforward numerical integration techniques, this phenonema makes it possible to find asymptotic and simple approximate solutions for $y(x, \rho)$ in these extremes. For example, the asymptotic solution for $y(x, \rho)$ for large x is

$$y(x, \rho) \sim \frac{\rho}{\sqrt{2\pi\left[x + \frac{(\rho^2 - 1)}{2}\right]}} \tag{24}$$

The conditions for which this expression is accurate to a given value are summarized in Table 4. These conditions were determined by comparison with exact numerically determined values.

The limiting form for $y(x, \rho)$ as ρ becomes small is $y(x, \rho) \rightarrow \exp(-2x)$. Combining this result with the asymptotic form yields the following approximation, which is accurate for all x to at least 1 percent for $\rho \leq 10^{-4}$,

Table 4. Conditions of Accuracy for the Asymptotic Solution for $y_L(x, \rho)$

Accuracy (%)	Minimum x		
0.01	$x \geq 1300$	and	$x \geq 85.0\rho^2$
0.1	130.0		$8.7\rho^2$
1.0	14.0		$2.5\rho^2$
10.0	5.3		$0.33\rho^2$

$$y(x, \rho) \simeq e^{-2x} + \frac{\rho}{\sqrt{2\pi x}} \quad . \tag{25}$$

The rapid changeover from the dominance of the first term to the dominance of the second is evident in Fig. 1b. Note that, for $\rho = 1$, $y(x, \rho)$ is the same as for the Curtis-Godson approximation, or, equivalently, $y(x, 1) = df(x)/dx$ by equation (23).

B. SOLUTION FOR $\bar{y}_L(x, \rho)$ FOR AN EXPONENTIAL LINE-INTENSITY DISTRIBUTION

The integral of equation (21b) can be evaluated in closed form by the method of residues. Since the integrand is even in θ, the limit of integration can be extended to $\theta = 2\pi$. By introducing the complex variable $z = e^{i\theta}$, the integral can be transformed (for $\rho \neq 1$) into

$$y(x, \rho) = \frac{8\rho}{i\pi(\rho^2 - 1)\, x^2} \oint_C \frac{z^2 dz}{\left[z^2 + 2\left(\frac{\rho^2 + 1}{\rho^2 - 1}\right) z + 1\right]\left[z^2 + 2\left(\frac{1 + x}{x}\right) z + 1\right]^2} \quad , \tag{26}$$

where the contour C is the unit circle about $z = 0$. The integrand has first-order poles at

$$z_1 = \frac{1 - \rho}{1 + \rho} \quad , \qquad z_2 = \frac{1 + \rho}{1 - \rho} \tag{27a, b}$$

and second-order poles at

$$z_3 = -\frac{1}{x}\left[(1 + x) - \sqrt{1 + 2x}\right] \quad , \tag{27c}$$

$$z_4 = -\frac{1}{x}\left[(1 + x) + \sqrt{1 + 2x}\right] \quad . \tag{27d}$$

Only the poles z_1 and z_3 lie within the contour C. The residue at $z = z_1$ is

$$A_{-1}^{(1)} = \frac{z_1^2}{(z_1 - z_2)(z_1 - z_3)^2(z_1 - z_4)^2} \quad . \tag{28a}$$

The residue at $z = z_3$ can be written

$$A_{-1}^{(3)} = \frac{z_3}{(z_3 - z_1)^2(z_3 - z_2)^2(z_3 - z_4)^3}\left[z_3(z_1 + z_2)(z_3 + z_4) - 2\left(z_3^3 + z_1 z_2 z_4\right)\right] \quad . \tag{28b}$$

Thus, the solution for $y(x, \rho)$ is

$$y(x, \rho) = \frac{16\rho}{(\rho^2 - 1)x^2}\left[A_{-1}^{(1)} + A_{-3}^{(3)}\right] \quad . \tag{29}$$

The solution is too complicated to be written out explicitly in terms of x and ρ.

When $\rho = 1$, the resultant integral is

$$y(x, 1) = \frac{2}{i\pi x^2}\oint_C \frac{z\,dz}{\left[z^2 + 2\left(\frac{1 + x}{x}\right) + x\right]^2} \quad . \tag{30}$$

Thus, only the second-order pole at z_3 is relevant. The resultant residue is

$$A_{-1}^{(3)} = \frac{-(z_3 + z_4)}{(z_3 - z_4)^3} \tag{31}$$

and the solution for $y(x, \rho)$ in terms of x is

$$y(x, 1) = \frac{1 + x}{(1 + 2x)^{3/2}} \quad . \tag{32}$$

As a check, note that this expression is the same as for the Curtis-Godson approximation, i.e., $y(x, 1) = df_e(x)/ds$.

If the contour integration technique is applied to the function $y_L(x, \rho)$ for an isolated Lorentz line, it is found that the integrand has an essential singularity at $z = 0$ from a term of the form $e^{-x/2z}$. The residue for such a singularity can be obtained only from a Laurent expansion of the integrand around the singularity. Unfortunately, this expansion procedure is quite complicated and eventually yields the residue in the form of an infinite series. Lindquist* reports that he has obtained a solution for this integral in the form of an infinite summation of Bessel functions.

C. NUMERICAL INTEGRATION OF $y_D(x, \rho)$

The integrand of the integral of equation (16b) has a single maximum at $z = 0$ whenever $x\rho^2 \leq 1$ and a single maximum at $z_0 = \rho^{-1}\sqrt{\ln(x\rho^2)}$ whenever $x\rho^2 > 1$. The integral was evaluated numerically in a manner similar to the evaluation of $y_L(x, \rho)$. A value of $z = z_m$ was determined such that the integral could be accurately written as

$$y(x, \rho) = \frac{2}{\sqrt{\pi}} \int_0^{z_m} e^{-z^2 - xe^{-\rho^2 z^2}} + \left\{1 - \operatorname{erf}(z_m)\right\} \quad . \tag{33}$$

For an absolute accuracy less than ϵ, z_m should satisfy

$$z_m > \frac{1}{\rho}\sqrt{\ln\left(\frac{x}{\epsilon}\right)} \quad .$$

*G. H. Lindquist, private communication.

For $x\rho^2 \leq 1$, the integral was evaluated by numerical integration between $z = 0$ and $z = z_m$ with the error function remainder added. For $x\rho^2 > 1$, the integrals for the regions $z = 0$ to $z = z_0$ and $z = z_0$ to $z = z_m$ were evaluated separately and then added along with the remainder term. The data in Table 2 are accurate to 1 part in 10^6 or better. For $\rho = 1$, $y(x, \rho) = dg(x)/dx$.

A series solution for $y(x, \rho)$ can be obtained by writing the integrand as a product of two exponential terms, expanding the term involving x and ρ into a power series, interchanging the order of summation and integration, and performing the resulting elementary integration with respect to z. The result is

$$y(x, \rho) = \sum_{n=0}^{\infty} \frac{(-x)^n}{(n+1)!\sqrt{1+n\rho^2}} \quad . \tag{34}$$

This expression is useful for calculating $y(x, \rho)$ for small values of x.

The limiting form for $y(x, \rho)$ as ρ becomes small is $y(x, \rho) \rightarrow e^{-x}$. For very large x and $x\rho^2 > 1$, the first term of the asymptotic expansion for $y(x, \rho)$ is

$$y(x, \rho) \sim \frac{\sqrt{2}}{(x\rho^2 e)^{1/\rho^2}} \frac{1}{\sqrt{\ln(x\rho^2)}} \quad . \tag{35}$$

This expression is useful for evaluating $y_D(x, \rho)$ for $x \gtrsim 100$ and $\rho \lesssim 2$.

D. NUMERICAL SOLUTION FOR $\bar{y}_D(x, \rho)$ FOR AN EXPONENTIAL LINE-INTENSITY DISTRIBUTION

The consideration of the integral of equation (22b) is almost identical to that for $y_D(x, \rho)$. The integrand has a single maximum at $z = 0$ for

$x(2\rho^2 - 1) \leq 1$ and a single maximum at $z_0 = \rho^{-1}\sqrt{\ln[x(2\rho^2 - 1)]}$ for $x(2\rho^2 - 1 > 1$. The integral can be written as a definite integral between the limits $z = 0$ and $z = z_m$ plus an error function remainder term to an absolute accuracy ϵ for

$$z_m > \frac{1}{\rho}\sqrt{\ln\left(\frac{2x}{\epsilon}\right)} \quad .$$

A series expansion for $x \leq 1$ can be obtained as

$$y(x, \rho) = \sum_{n=0}^{\infty} \frac{(n + 1)(-x)^n}{\sqrt{1 + n\rho^2}} \quad . \tag{36}$$

A useful approximation for $\rho \lesssim 0.5$ is

$$y(x, \rho) = \frac{1}{(1 + x)^{3/2}\sqrt{1 - x(2\rho^2 - 1)}} \quad .$$

This approximation is accurate to at least 2 percent for all x. As ρ goes to zero, $y(x, \rho) \rightarrow (1 + 2x)^{-1}$. An asymptotic solution (though not too useful) for large x is

$$y(x, \rho) \sim \frac{1}{2\rho^2} \frac{(2\rho^2 - 1)^{3/2}}{\left[x(2\rho^2 - 1)\right]^{1/\rho^2}} \frac{1}{\sqrt{\ln[x(2\rho^2 - 1)]}} \quad . \tag{37}$$

Finally, $y(x, 1) = dg_e(x)/dx$.

The tabular interpolation for $y(x, \rho)$ is facilitated for this case by interpolating with respect to the parameter $\alpha = \rho/(1 + \rho)$, which has limits 0 and 1, respectively, for $\rho = 0$ and $\rho = \infty$.

REFERENCES

1. G. H. Lindquist and F. S. Simmons, "A Band Model Formulation for Very Nonuniform Paths," J. Quant. Spectr. Radiative Transfer 12, 807 (1972).

2. S. S. Penner, Quantitative Molecular Spectroscopy and Gas Emissivities, Addison-Wesley, Reading, Mass. (1959).

3. G. H. Goody, Atmospheric Radiation I. Theoretical Basis, Oxford Clarendon Press, Oxford (1964).

4. W. Malkmus, "Random Lorentz Band Model with Exponential-Tailed S^{-1} Line Intensity Distribution Function," J. Opt. Soc. Am. 57, 323 (1967).

5. W. Malkmus, "Random Band Models with Lines of Pure Doppler Shape," J. Opt. Soc. Am. 58, 1214 (1968).

6. A. Goldman, "On Simple Approximations to the Equivalent Width of Lorentz Lines," J. Quant. Spectr. Radiative Transfer 8, 829 (1968).

7. C. D. Rodgers and A. P. Williams, "Integrated Absorption of a Spectral Line with the Voigt Profile," J. Quant. Spectr. Radiative Transfer 14, 319 (1974).

8. H. Margenau and G. H. Murphy, The Mathematics of Physics and Chemistry, Van Nostrand, Princeton, N. J. (1964).